

Assessment of conventional HVDC line protection methods for modular multilevel converter based HVDC line

Mohammedirfan I. Siddiqui¹ , Bhargav Y. Vyas^{2,*} 

¹Research Scholar, Electrical Engineering Department, Gujarat Technological University, Ahmedabad, India.

²Electrical Engineering Department, L.E. College of Engineering, Morbi, India.

*Corresponding author: bhargavonline@gmail.com

Original Research

Received:
10 June 2024

Revised:
02 December 2024

Accepted:
21 December 2024

Published online:
01 March 2025

© 2025 The Author(s). Published by the OICC Press under the terms of the [Creative Commons Attribution License](https://creativecommons.org/licenses/by/4.0/), which permits use, distribution and reproduction in any medium, provided the original work is properly cited.

Abstract:

The Modular Multilevel Converter (MMC) HVDC system is becoming increasingly significant in contemporary power grids as power electronics technology continues to evolve. It is essential to provide protection in large DC circuits to maintain stability and security during faults. This paper presents a comparative analysis of the travelling wave-based protection schemes of PMGMW and CBTW, which were originally developed for LCC HVDC systems and have been adapted for a two-terminal MMC HVDC system. In order to assess fault resistance endurance, fault identification accuracy, and processing time under a variety of fault conditions, simulations were conducted in PSCAD/EMTDC. The results suggest that Pole Mode Ground Mode Wave's (PMGMW) scheme is more resilient to high resistance faults, maintaining accuracy at fault resistances of up to 100 Ω , while Change in Backward Travelling wave's (CBTW) scheme is less resilient to high resistance faults but demonstrates quicker fault identification with reduced processing time. Consequently, this investigation further solidifies the insights into the improvement of current protection systems for MMC HVDC applications.

Keywords: High voltage direct current transmission; Line commutated converter; Modular multi-level converter; Travelling wave based protection; DC circuit breaker

1. Introduction

In contrast to Line Commutated Converter (LCC) HVDC systems, Voltage Source Converter (VSC) HVDC grids exhibit significantly higher DC fault propagation speeds, potentially causing extensive system damage within milliseconds [1]. Protection for DC lines in LCC-HVDC transmission systems has been extensively developed and holds significant practical application knowledge, offering valuable perspectives for VSC-HVDC grids. For DC lines in LCC-HVDC systems, single-ended travelling wave-based protection techniques are now the main means of protection [2–5]. Electrical energy is believed to propagate through waves as per the electromagnetic field theory. Along the transmission line, voltage and current waves move under both healthy and unhealthy circumstances. But in the event of a fault, travelling waves due to the fault originate and propagate at the speed of light along each end of the line, carrying important data regarding the fault. HVDC line

protection can leverage the fault-generated transient travelling waves to meet the need for quick response. The pole mode wave and its rate of change are the main tools used by PMGMW travelling wave-based DC protection approach to identify the damaged pole [2, 3]. Although this method can provide comprehensive protection for the entire line, it still requires further improvements to enhance its resilience against high transition resistance and disturbance. CBTW has a protection strategy that utilizes the integration of backward travelling waves to enhance its anti-interference capability. However, this approach may also result in slower acting speeds [4]. Despite these limitations, this protection method represents a significant step forward in safeguarding transmission lines and reducing the risk of electrical failures.

With continued research and development, it is possible to further enhance the effectiveness of this technique and improve the overall reliability of power grids. [5]. More recent studies have concentrated on improving DC line protection

for VSC-HVDC grids, building on protection techniques created for LCC-HVDC systems. Reference [6] investigated a protection criterion for VSC-HVDC grids based on the Rate of Change of Voltage (ROCOV), achieving faster operation through increased sampling frequency. The resilience of ROCOV-based protection in situations with significant transition resistance, however, was not covered in the study. In reference [7], researcher proposed a protection scheme utilizing voltage and current wavelet analysis and the rate of change in voltage and current wavelet analysis; however, it lacks theoretical underpinning. Moreover, it cannot provide complete line protection as it does not account for boundary elements. In Reference [8], a protection scheme is introduced that uses Rate of Change of Voltage (ROCOV) at the line side of the DC reactor for fault detection and location. The scheme effectively prevents backward faults by comparing ROCOV on both sides of the DC reactor. In reference [9], author introduces a protection strategy that employs the rate of change of DC reactor voltage. This protection scheme is intended for use in a meshed multi-terminal HVDC grid in which DC reactors are situated at both extremities of each line. A non-unit protection system depending on travelling wave reflection at inductive terminations is presented in Reference [10]. Using voltage magnitude and its derivative, this method separates forward internal and external faults, eliminating backward faults depending on current derivative analysis. The aforementioned studies explored the implementation of traveling wave protection in VSC HVDC grids. Each of these single-ended protection techniques, nevertheless, are unable to discriminate between severe external faults and internal high impedance faults. A protective strategy relying on the ratio of transient voltages was developed in Reference [11]. It uses remote-end data to handle high-resistance problems. For DC grids based on Modular Multilevel Converters (MMCs), Reference [12] presented a transient voltage-based protection concept. Indeed, directional criteria are crucial in majority of the previously mentioned single sided protections to mitigate backward faults. Currently, directional criteria in DC systems chiefly rely on variations in DC current (Δi) or its rate of change ($\frac{di}{dt}$) [9–13]. Similarly, the fault is determined to be forward when the di/dt value used in the direction criterion is above a positive threshold. Nevertheless, owing to the charging and discharging of distributed line capacitors, $\frac{di}{dt}$ swings among positive and negative values for both forward and backward faults. The steadiness is compromised by this variability [13]. Thus, ongoing research is essential for developing direction criteria that are fast and reliable. None of these methods for protecting VSC HVDC transmission lines have been implemented in practice. This paper implements conventional PMGMW and CBTW protection of LCC HVDC systems specifically for a two-terminal MMC HVDC system. Both protection schemes are analysed and compared through simulations, considering factors like fault resistance, fault distance, internal and external faults, and frequency-dependent overhead lines. The results indicate that PMGMW protection exhibits greater resilience against fault resistance endurance compared to CBTW. Both PMGMW and CBTW use change

rate criteria to differentiate between internal and external faults. CBTW protection uses change in backward travelling wave to select fault lines, while PMGMW utilizes ground wave change rate for the same purpose. Addressing existing limitations of traveling wave protection schemes, an improvement points are recommended based on these criteria. This research paper investigates the application of existing travelling wave-based protection systems, originally designed for Line Commutated Converter (LCC) HVDC grids, to a two-terminal Modular Multilevel Converter (MMC) HVDC system. The key contributions of this research are as follow: The paper compares the performance of PMGMW and CBTW travelling wave-based protection systems through simulations. It analyses how each system identifies fault type and location using travelling wave characteristics. While these protection systems were developed for LCC-HVDC, the research explores their effectiveness when adapted for MMC-HVDC grids. This is valuable because MMC-HVDC systems have different fault propagation characteristics compared to LCC-HVDC. The simulations consider various factors that can impact protection performance, including transition resistance, fault distance, internal and external faults, and frequency dependence of overhead line. This allows for a comprehensive understanding of how these systems respond under different fault scenarios. Based on the analysis of simulation results, the paper identifies the limitations of both PMGMW and CBTW protection systems. It suggests potential areas for improvement to enhance their effectiveness in MMC-HVDC applications. This provides valuable insights for future research and development of MMC-HVDC protection schemes.

The swift advancement of HVDC technology, particularly the transition from Line Commutated Converter (LCC) to Modular Multilevel Converter (MMC) based systems, introduces novel difficulties in detecting and safeguarding against faults. Conventional safety methods intended for from Line Commutated Converter (LCC) High Voltage Direct Current (HVDC) systems may have difficulties in dealing with the distinct issues presented by Modular Multilevel Converter (MMC) HVDC systems. These problems include the rapid spread of faults and the absence of inherent zero-crossings in DC faults. The objective of this research is to explore possible modification and augment existing protection strategies in order to provide robust and rapid fault detection in MMC HVDC systems. The effective management of high fault resistance and the differentiation between internal and exterior faults provide a notable research gap. In order to enhance grid stability and minimise the likelihood of system-wide failures, it is imperative to address these deficiencies. These findings may guide further evolution of secure and fast-acting protection systems for ensuring the stability and security of MMC-HVDC power grids.

The subsequent sections of this paper are organized as follows: Section 2 discusses the two-terminal MMC HVDC system testing, Section 3 provides a detailed presentation of travelling wave based protection of PMGMW and its simulation result, Section 4 showcases protection scheme of CBTW and its simulation results, Section 5 shows compara-

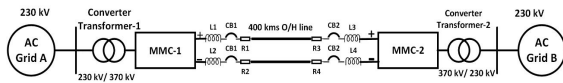


Figure 1. 2- Terminal Symmetrical Monopole MMC HVDC.

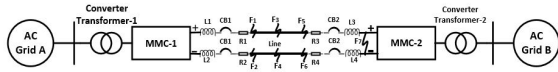


Figure 2. 2- Terminal Symmetrical Monopole MMC HVDC with fault location.

tive analysis of PMGMW and CBTW, Section 6 showcases summary for protection scheme and Section 7 shows concluding remarks.

2. System layout

Fig. 1 shows circuit layout of a symmetrical monopole two-terminal MMC HVDC system, where each converter uses full bridge MMC. A monopole HVDC system typically consists of a single/two high-voltage DC line that carries the transmission between the converter stations. For a typical monopole MMC HVDC line, at least two DC circuit breakers are required-one at each converter station. Additional breakers may be included based on specific system needs and protection strategies. In this configuration, DC circuit breaker are installed at positive and negative pole at each converter station. The DC circuit breaker CB1 and CB2 adopts the hybrid DCCB topology presented in [14]. For protection and to trip the DC circuit breakers, relays R1 and R2 are deployed at converter station-1, and relays R3 and R4 at converter station-2. The inductors are positioned on the DC line side of DCCBs to control the rate of rise of fault currents and serve as barriers for DC lines, offering high impedance paths for high-frequency components.

On DC transmission lines, pole to pole faults (PTP) and pole to ground faults (PTG) are frequent. Comprehensive analysis and fault current calculations are given in references [15] and [16]. Article [17] introduces a resilient non unit traveling wave protection (TWP) system designed to identify DC fault areas and discriminate fault types under high impedance fault conditions. Article [18] offers an in-depth review and analysis of the control and protection mechanisms utilized in the MMC-based multi-terminal direct current (MTDC) system. When a PTP fault occurs, the DC terminal voltage on the affected line quickly drops to zero, accompanied by a substantial surge in current in the line. When a PTG/NTG fault occurs, the voltage at the faulted pole drops to zero, while at the healthy pole, it becomes doubles to the rated voltage. Depending on the fault feature, DC fault identification criteria can be developed using time domain strategies. However, in case of high resistance PTG/NTG fault, the variations in line voltage and current may not be substantial.

3. Pole mode-ground mode wave (PMGMW) travelling wave protection

3.1 Basic principle and protection criteria

In recent years, research has focused on developing protections for the DC lines in VSC-HVDC systems, drawing insights from protections used in LCC HVDC systems. Protection of LCC-HVDC system by PMGMW is applied to two terminal VSC HVDC system. In this method, pole mode and ground mode components are calculated as follow,

$$P = I_{d1}Z_{c1} - U_{d1} \quad (1)$$

$$G = I_{d0}Z_{c0} - U_{d0} \quad (2)$$

Where I_{d1} , U_{d1} and Z_{c1} represent the current of line mode, voltage of line mode and impedance of line mode respectively. I_{d0} , U_{d0} and Z_{c0} represent the current of ground mode, voltage of ground mode and impedance of ground-mode respectively. The pole mode element (P) and ground mode element (G) signify the backward-traveling waves of the line and ground modes, respectively [19]

$$\begin{pmatrix} I_{d0} \\ I_{d1} \end{pmatrix} = Q^{-1} \begin{pmatrix} I_P \\ I_N \end{pmatrix} \quad (3)$$

$$\begin{pmatrix} U_{d0} \\ U_{d1} \end{pmatrix} = Q^{-1} \begin{pmatrix} U_P \\ U_N \end{pmatrix} \quad (4)$$

Where U_P and I_P are positive pole voltage and current, while U_N and I_N are negative pole voltage and current.

$$Q = \frac{1}{\sqrt{2}} \begin{bmatrix} 1 & 1 \\ 1 & -1 \end{bmatrix} \quad (5)$$

$$Z_{c0} = \sqrt{\frac{(Z_s + Z_m)}{(Y_s + Y_m)}} \quad (6)$$

$$Z_{c1} = \sqrt{\frac{(Z_s - Z_m)}{(Y_s - Y_m)}} \quad (7)$$

Where Z_s and Z_m are the self and mutual impedance of line, Y_s and Y_m are the self and mutual admittance of line. $Z_{c1} = 250 \Omega$, $Z_{c0} = 500 \Omega$ for two conductor flat tower and symmetrical configured 3 bundled sub conductor. Travelling wave velocity is 2.879×10^5 km/s.

Upon a fault in line, the traveling wave emanates from the fault point, reaching both ends of line and traveling in opposite direction as well. Due to fault, many parameters like DC Voltage, DC current etc. of the line change quickly. PMGMW travelling wave protection checks four criteria to recognize the fault on line.

- 1) The change in pole mode wave (ΔP)
- 2) Rate of change of pole mode wave $\frac{dP}{dt}$
- 3) Change in ground mode wave (ΔG)
- 4) Rate of change of ground mode wave $\frac{dG}{dt}$ [20].

To assess the protection algorithm a 2-terminal MMC HVDC system is emulated in PSCAD/EMTDC and its all relevant criteria shown in Fig. 3.

All these criteria are compared with various thresholds as follow [21].

$$\begin{cases} \frac{dP}{dt} > \Delta_1 \\ \Delta P > \Delta_2 \\ \frac{dG}{dt} > \Delta_3 \\ \Delta G > \Delta_4 \end{cases} \quad (8)$$

$\Delta_1 - \Delta_4$ are thresholds value which are decided by various simulation results. ΔP and $\frac{dP}{dt}$ are used to determine internal and external fault. If $\frac{dP}{dt} < \Delta_1$ and $\Delta P < \Delta_2$, then fault is identified as an external fault. All four criteria are shown in Fig. 3.

Upon the occurrence of the fault, the values of the two parameters increase significantly. This is the heart of PMGMW travelling wave protection system. There are many filters connected at terminal end which will work as boundary components. During external fault, the value of ΔP and $\frac{dP}{dt}$ will be smaller due to boundary components.

3.2 Implementation of protection scheme

To eliminate unnecessary activations of the protection scheme during standard operations and certain external faults, a start-up element is used to activate the scheme. When fault takes places, DC voltage reducing drastically hence voltage derivative criteria ($\frac{dU}{dt}$) is employed. Once start up element is activated then it will start to perform various calculations.

Step-1: Obtain sampled voltage and current data and calculate voltage derivative. Compare it with threshold value.

Step-2: Perform modal analysis and Calculate zero mode voltage (U_{d0}), pole mode voltage (U_{d1}), zero mode current (I_{d0}) and pole mode current (I_{d1}) by using Eq. (3) and Eq. (4).

Step-3: Find out Pole mode component (P) and Ground Mode component (G) by using Eq. (1) and Eq. (2). And also calculate rate of change of pole mode component ($\frac{dP}{dt}$) and change in pole mode component (ΔP). The backward traveling wave in line mode is represented by the pole mode (P) component, while in ground mode it is represented by the ground mode (G) component.

Step-4: Compare ($\frac{dP}{dt}$) and (ΔP) with threshold values Δ_1 and Δ_2 respectively. If criteria is satisfied then it is termed as internal fault else external fault.

Step-5: Calculate and compare rate of change of ground mode wave ($\frac{dG}{dt}$) and Change in ground mode wave (ΔG) with thresholds Δ_3 and Δ_4 respectively to identify PTP fault and PTG/NTG fault.

Step-6: At last, check and compare the value of Ground mode (G) with Δ_5 , Δ_6 and Δ_7 to identify PTP fault, PTG fault and NTG fault respectively. Fig. 3 illustrates all the aforementioned steps as a flowchart. The threshold values given as follow are carefully selected to ensure that the protection algorithm activates during high-impedance internal faults and remains inactive during external faults.

- 1) $G > \Delta_5$ -Positive Pole to Ground Fault (PTG)
- 2) $G < \Delta_6$ -Negative Pole to Ground Fault (NTG)
- 3) $-\Delta_7 \leq G \leq \Delta_7$ -Pole to Pole Fault (PTP)

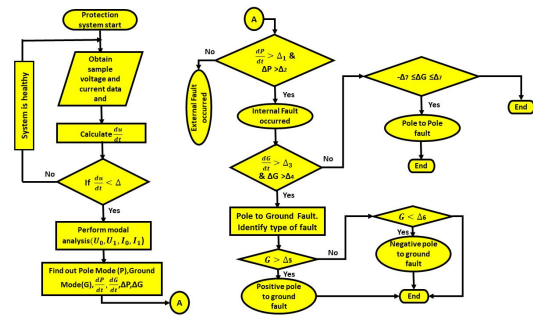


Figure 3. Flow Chart of PMGMW method].

3.3 Simulation and results

The simulation studies were conducted using PSCAD/EMTDC, focusing on a two-terminal MMC HVDC system with ± 320 kV, 1.5 kA, 1000 MW capacity proposed by CIGRE B4 57. The chosen parameters include fault resistances ranging from 0.01 Ω to 100 Ω , fault distances from 0 to 400 km, and various types of faults such as pole-to-pole (PTP), positive pole-to-ground (PTG), and negative pole-to-ground (NTG) faults. The simulation modes were designed to capture the dynamic response of the system under both internal and external fault conditions, with a sampling frequency of 20 kHz. Fault occurrence times were set at 2 seconds into the simulation to ensure steady-state conditions prior to fault initiation. The results were analysed to evaluate the protection schemes' effectiveness in terms of fault detection speed, accuracy, and reliability under varying fault conditions. $\Delta = -1.2 \times 10^3$ kV/s, $\Delta_1 = 4 \times 10^3$ kV/s, $\Delta_2 = 0.25$ kV, $\Delta_3 = 1 \times 10^3$ kV/s, $\Delta_4 = 0.5$ kV, $\Delta_5 = 100$ kV, $\Delta_6 = -100$ kV, $\Delta_7 \approx 16$ kV.

The essential parameters of the MMC HVDC system are outlined in Table 1.

Fig. 4 shows the response of the DC voltage of MMC HVDC line for faults arising at various locations with varying resistances. The simulated MMC HVDC system in this work is a symmetrical monopole structure consisting of full-bridge sub-modules. The rating of each converter station is 1000 MW, together with a DC voltage of ± 320 kV and a DC current capacity of 1.5 kA. Within each arm, the system utilises 76 sub-modules, each equipped with a 2800 μ F capacitor. The DC line overhead line is of 400 kms with a resistance rating of 0.010605 /km and an inductance rating of 0.280 mH/km. Individual DC circuit breakers are strategically placed at every converter station, employing a hybrid DCCB architecture to ensure fault isolation. The use of smoothing inductances of 50 mH serves to restrict the increase of fault current. In addition to protective activation relays, the simulation model incorporates current limiting inductors on the DC line side to serve as boundaries for high-frequency components. This comprehensive modelling guarantees precise depiction of the behaviour of the MMC HVDC system during fault situations, thereby enabling the evaluation of the simulated protection programs.

Table 1. System Parameters.

Rated Capacity	1000 MW, 1.5 kA
Rated DC Voltage	±320 kV
Grid side AC Voltage	230 kV
Submodule numbers per arm	76
Submodule Capacitor	2800 μF
Arm reactor	50 mH
Effective resistance of the dc line	0.010605 Ω/km
Effective inductance of the dc line	0.280 mH/km
Length of Line	400 kms
Transformer Rating	1000 MVA, 230/370 kV, $X_r=0.1$ PU
Smoothing Inductance	50 mH
Converter Rating	1000 MVA
Converter Reactor	0.00125 H
Converter Resistance	0.0005 Ω

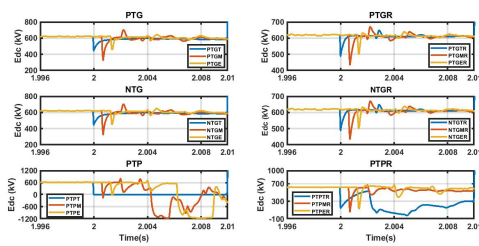


Figure 4. DC voltage during various faults.

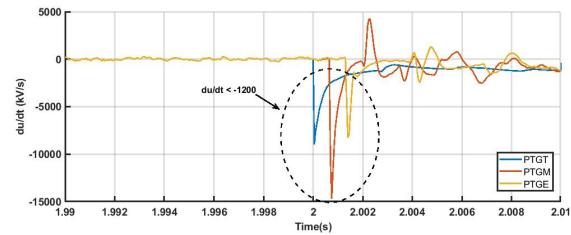


Figure 6. ROCOV ($\frac{du}{dt}$) for PTGT, PTGM and PTGE.

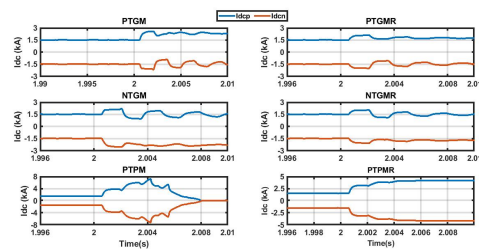


Figure 5. I_{dcp} and I_{dcn} during MID point fault.

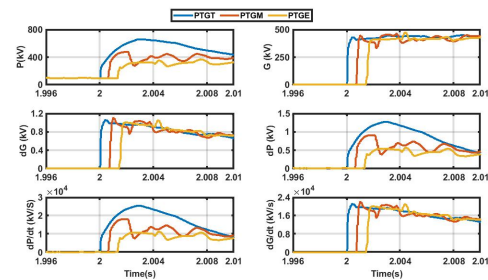


Figure 7. P , G , ΔG , ΔP , $\frac{dP}{dt}$ and $\frac{dG}{dt}$ for PTGT, PTGM, PTGE fault.

Case-1: positive pole to ground fault with fault resistance $R_g = 0.01 \Omega$ and $R_g = 100 \Omega$

As shown in Fig. 2, PTG faults are taking place near terminal of MMC-1 denoted as F_1 , MID point of transmission line (F_3) and end point of line (F_5). Fault produced travelling waves will travel from fault point to both side of converters. Relays R_1 and R_2 will check the ROCOV (rate of change of voltage) criteria and it will identify the fault once the value of $\frac{du}{dt} < \Delta$. As shown in Fig. 6, ROCOV has depicted for positive pole to ground fault at terminal (PTGT), positive pole to ground fault at mid point (PTGM) and positive pole to ground fault at end point (PTGE) of transmission line.

Fig. 4 depicts the DC voltage of the line, accounting for several faults at various locations with differing fault resistances. Fig. 5 depicts the positive (I_{dcp}) and negative (I_{dcn}) pole current during positive pole to ground fault at mid point (PTGM), positive pole to ground fault at mid point with R_g (PTGMR), negative pole to ground fault at mid point (NTGM), negative pole to ground fault at mid point with R_g (NTGMR), pole to pole fault at mid point

(PTPM), pole to pole fault at mid point with R_g (PTPMR). The identification of as an internal fault, as illustrated in Fig. 7 is based on the change in pole mode component (ΔP) and its derivative ($\frac{dP}{dt}$) exceeding the pre-set thresholds Δ_2 and Δ_1 . The values of ΔG and $\frac{dG}{dt}$ exceed their respective threshold values, prompting the PMGMW protection scheme to classify it as positive pole to ground fault and initiate a tripping signal to the HVDC circuit breaker. Now As shown in Fig. 2, consider PTG fault with $R_g = 100 \Omega$ are taking place near terminal of MMC-1 denoted as F_1 , MID point of transmission line (F_3) and end point of line (F_5). The conditions based on the change in pole mode component (ΔP) and derivative of pole mode component ($\frac{dP}{dt}$) is determining the PTGTR (positive pole to ground fault at terminal with $R_g = 100 \Omega$), PTGMR (positive pole to ground fault at MID point with $R_g = 100 \Omega$) and PTGER (positive pole to ground fault at end point with $R_g = 100 \Omega$) internal fault as they surpass the set threshold values Δ_2 and Δ_1 respectively. The value of ΔG and $\frac{dG}{dt}$ are also beyond the predefined threshold values which are depicted in Fig. 8. So PMGMW protection scheme is able to identify

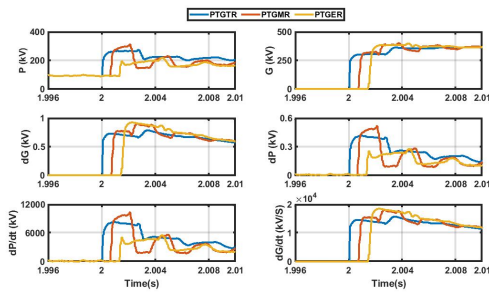


Figure 8. P , G , ΔG , ΔP , $\frac{dP}{dt}$ and $\frac{dG}{dt}$ for PTGT, PTGM, PTGE fault.

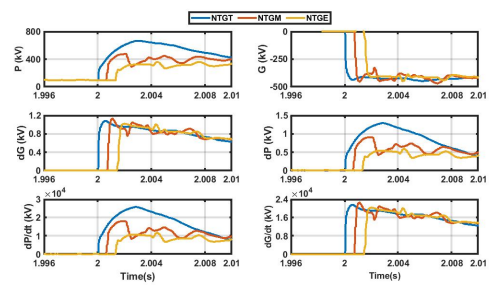


Figure 10. P , G , ΔG , ΔP , $\frac{dP}{dt}$ and $\frac{dG}{dt}$ for NTGT, NTGM, NTGE fault.

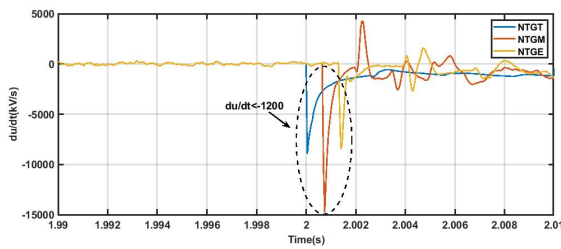


Figure 9. ROCOV ($\frac{du}{dt}$) for NTGT, NTGM and NTGE.

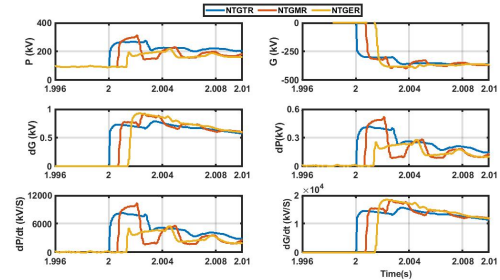


Figure 11. P , G , ΔG , ΔP , $\frac{dP}{dt}$ and $\frac{dG}{dt}$ for NTGTR, NTGMR, NTGER fault.

high resistance fault at far end (400 kms).

Case-2: negative pole to ground fault with fault resistance $R_g = 0.01 \Omega$ and $R_g = 100 \Omega$

As shown in Fig. 2, The line is perturbed by NTG fault at near terminal of MMC-1 denoted as F_2 , MID point of transmission line (F_4) and end point of line (F_6). Protection algorithm of relays R_1 and R_2 will check $\frac{du}{dt} < \Delta$ which is shown in Fig. 9 for NTGT (Negative pole to ground fault at terminal), NTGM (Negative fault to ground fault at MID point) and NTGE (Negative pole to ground fault at End point) then it will detect it as internal fault as per step no-4 of flow chart. Value of ΔG and $\frac{dG}{dt}$ are greater than threshold values and hence it is recognized as pole to ground fault. At last, it is decided about type of fault by checking the parameter G as shown in Fig. 10.

As depicted in Fig. 2, consider a negative pole to ground fault with a resistance $R_g = 100 \Omega$ occurring at various locations: near the terminal of MMC-1 (F_2), at the middle point of transmission line (F_4), and at line’s endpoint (F_6). The detection condition based on the change in pole mode wave (ΔP) and derivative of pole mode component ($\frac{dP}{dt}$) effectively identify internal faults at the terminal (NTGTR), midpoint (NTGMR), and endpoint (NTGER) of the line. These faults are distinguished by values exceeding their respective pre-set thresholds Δ_2 and Δ_1 . Similarly, the values of ΔG and $\frac{dG}{dt}$ surpass their corresponding threshold values, as shown in Fig. 11. Consequently, the PMGMW protection scheme can also recognize high-resistance faults even at a considerable distance, such as 400 km away.

Case-3: pole to pole fault

As depicted in Fig. 2, the line experiences pole-to-pole faults at various points: near terminal of MMC-1 (locations F_1 and F_2), at the midpoint of the transmission line (locations F_3 and F_4), and at the line’s endpoint (locations F_5 and F_6). Relays R_1 and R_2 will detect these faults by performing

the ROCOV (rate of change of voltage) criteria ($\frac{du}{dt} < \Delta$) as show in Fig. 12. Additionally, the fault is detected as internal if the change in pole mode wave (ΔP) and its derivative ($\frac{dP}{dt}$) exceed their respective threshold values, as illustrated in Fig. 13. Since this is not a ground fault, ΔG and $\frac{dG}{dt}$ do not exceed their threshold limits. Instead, the value of G remains within the threshold range of $-\Delta_7$ to Δ_7 , confirming it as PTP fault, as depicted in Fig. 13.

Case-3: pole to pole fault external

As depicted in Fig. 2, an external PTP faults (F_7) eventuate at the terminal of converter station-2. Relays R_1 and R_2 should correctly recognize this fault as external and refrain from operating, as this is not internal fault. As shown in Fig. 14, value of ΔP and $\frac{dP}{dt}$ are greater than threshold and value of G also falls between $-\Delta_7$ to Δ_7 , confirming it as a PTP fault. Consequently, the PMGMW protection algorithm can not detect external fault at considerable distance, such as 400 km away.

Table 2 presents the performance results of PMGMW traveling wave protection system for overhead lines, detailing fault identification criteria and internal/external differentiation across different fault types. It verifies that PMGMW TW protection scheme works for all type of in-

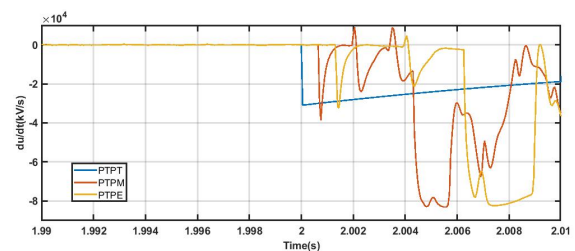


Figure 12. ROCOV ($\frac{du}{dt}$) for PTPT, PTPM and PTPE.

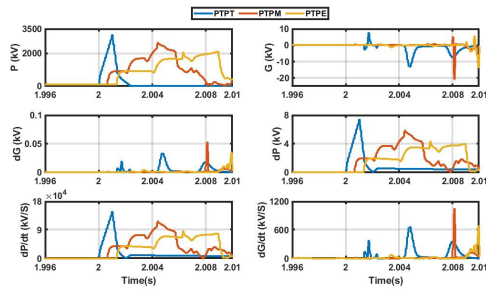


Figure 13. P , G , ΔG , ΔP , $\frac{dP}{dt}$ and $\frac{dG}{dt}$ for PTPT, PTPM, PTPE fault.

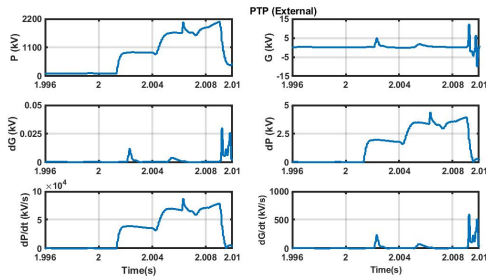


Figure 14. P , G , ΔG , ΔP , $\frac{dP}{dt}$ for External PTP fault.

ternal low/high impedance fault but it can not guarantee selectivity and reliability under external fault for particular two terminal MMC HVDC system. The main impact of fault distance on travelling wave protection is attenuation of amplitude and increased propagation time. Fault resistance also attenuates the amplitude of travelling waves. Therefore, increase in traveling wave arrival time will impact the amplitude of protection criteria.

4. Change in backward travelling wave (CBTW) protection

CBTW a traveling wave based protection operates on a distinctive operational principle. When a fault eventuate, the fault generated traveling wave moves towards protection location. As the wave propagates, the DC voltage monitored by the protection decreases rapidly. By calculating, the rate of change of voltage (ROCOV) and backward traveling wave $b(t)$ [$b(t) = \Delta I_d * Z_c - \Delta U_d$], the system can detect the dc fault. Overall, the CBTW protection system offers a sophisticated and effective solution to detect faults and maintain power system stability.

4.1 Basic principle and protection criteria

To establish protection, certain conditions must be fulfilled. In order to identify a fault, following steps must be taken: first, $\frac{du}{dt}$ must be less than a predetermined threshold value. Next, the integral value of $\Delta b(j) = b(j) - b(k)$ must be calculated for a duration of 10 milliseconds. Here, $b(k)$ denotes the most recent value of sample before fault, whereas $b(j)$ represents the value of sample taken at point j after the fault. If integral value exceeds a positive threshold, fault is categorized as PTG fault. Conversely, if integral value falls below negative threshold, fault is categorized as NTG fault. Forward travelling wave (FTW) and backward travelling wave (BTW) generated by fault can be calculated from

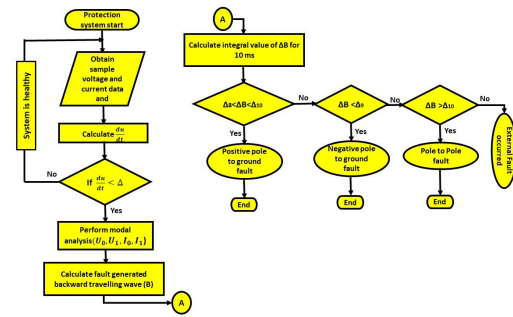


Figure 15. Flow Chart of CBTW method.

following equations,

$$F = Z_{c1} * \Delta I_1 + \Delta U_1 \tag{9}$$

$$B = Z_{c1} * \Delta I_1 - \Delta U_1 \tag{10}$$

Where ΔU_1 = change in pole mode voltage, ΔI_1 = change in pole mode current, Z_{c1} = Line mode impedance, F = Fault generated FTW, B = Fault generated BTW.

4.2 Implementation of protection scheme

A start-up element is incorporated to minimize the frequent activation of the protection system during healthy operating states and specific external disturbances. Upon the occurrence of a fault, DC voltage experiences a significant reduction, triggering the voltage derivative criterion ($\frac{du}{dt}$). Initiation of the start-up element initiates series of subsequent calculations to accurately address the fault condition.

Step-1: Obtain sampled voltage and current data and calculate voltage derivative. Compare it with threshold value.

Step-2: Perform modal analysis and Calculate zero mode voltage (U_{d0}), pole mode voltage (U_{d1}), zero mode current (I_{d0}) and pole mode current (I_{d1}) by using Eq. (3) and Eq. (4).

Step-3: Calculate fault generated backward travelling wave using Eq. (10).

Step-4: Compute the integral of ΔB for 10 milliseconds to classify the fault type.

Step-5: $\Delta_8 < \Delta B < \Delta_{10}$ then PTG fault $\Delta B < \Delta_9$ then NTG fault $\Delta B > \Delta_{10}$ then PTP fault $\Delta_8 = 0.5$ kV, $\Delta_9 = -0.01$ kV $\Delta_{10} = 1.5$ kV All these threshold values are decided based on system parameters and numerous simulation studies. All above mentioned steps are shown in Fig. 15.

4.3 Simulations and results

As discussed in the context of TW protection for PMGMW, all cases have been analysed for CBTW protection as well. This analysis focuses solely on ΔB waveforms, as other waveforms were already covered in the previous method. CBTW protection utilizes BTW instead of FTW because BTW reaches the relay location sooner after a fault occurs.

Case-1: PTG, NTG and PTP fault

Fig. 2 illustrates various faults occurring at various locations along the line: near terminal of MMC-1 (points F_1 and F_2), at the midpoint of transmission line (points F_3 and F_4), and at end of the line (points F_5 and F_6). When the ROCOV (rate of change of voltage) criterion ($\frac{du}{dt} < \Delta$) is met, relay

Table 2. Summary of PMGMW TW protection scheme.

Type of Fault	Location of Fault (kms)	Fault Resistance (R_g) in Ω	ΔP (kV) (0.25)	$\frac{dP}{dt}$ (kV/s) (4×10^3)	ΔG (kV) (0.5)	$\frac{dG}{dt}$ (kV/s) (1×10^3)	Ground Mode G (kV)	Pole Mode P (kV)	Correct Operation
Positive Pole to Ground (PTG)	0	0.01	1.2	25.3×10^3	0.98	20×10^3	440	651	Yes
	0	100	0.4	8×10^3	0.668	13.41×10^3	363	261	Yes
	200	0.01	0.9	17.5×10^3	1.06	21.3×10^3	452	462	Yes
	200	100	0.43	9.9×10^3	0.88	17.4×10^3	400	300	Yes
	400	0.01	0.56	11.33×10^3	1.07	21.6×10^3	476	367	Yes
	400	100	0.284	5.7×10^3	0.94	19×10^3	396	216	Yes
	External	0.01	0.53	10.7×10^3	1.08	21.6×10^3	438	350	No
Negative Pole to Ground (NTG)	0	0.01	1.28	25.6×10^3	1.12	22.4×10^3	-444	661	Yes
	0	100	0.418	8.37×10^3	0.74	15×10^3	-362	268	Yes
	200	0.01	0.87	17.5×10^3	1.1	22×10^3	-470	463	Yes
	200	100	0.5	9.9×10^3	0.89	17.8×10^3	-396	300	Yes
	400	0.01	0.54	11×10^3	0.91	18.5×10^3	-443	347	Yes
	400	100	0.26	5.2×10^3	0.84	16.7×10^3	-394	210	Yes
	External	0.01	0.55	11.1×10^3	1.08	21.6×10^3	-443	350	No
Pole to Pole (PTP)	0	0.01	6.02	120×10^3	0.01	28	≈ 0.892 to -5.73	2816	Yes
	200	0.01	5.56	98.5×10^3	0.0012	28	≈ 0.892 to -18.4	2279	Yes
	400	0.01	6.85	137×10^3	0.04	900	≈ 0.892 to 16	2055	Yes
	External	0.01	4.72	95×10^3	0.026	515	≈ 6 to -14	2150	No

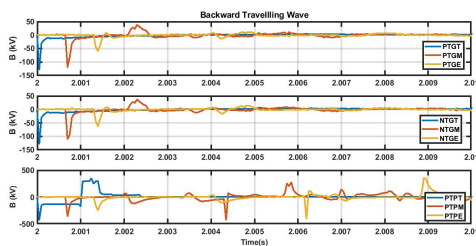


Figure 16. Fault generated BTW for PTG,NTG and PTP fault at terminal, mid point and end point.

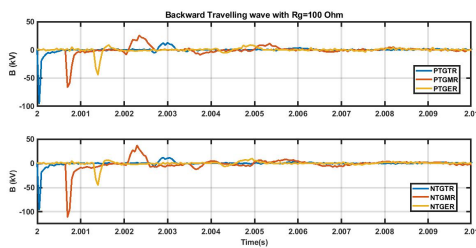


Figure 17. Fault generated BTW for PTG, NTG and PTP fault with $R_g = 100 \Omega$ at terminal, mid point and end point.

algorithms for R_1 and R_2 initiate modal analysis to identify pole mode and ground mode components. This analysis detects the backward traveling wave produced by the fault as shown in Fig. 16 and calculates integral value of ΔB for 10 ms, compares it against various thresholds to deduce whether the fault is an internal PTG fault, NTG fault, PTP fault, or an external fault.

Case-2: PTG and NTG fault with $R_g = 100 \Omega$

Fig. 2 illustrates various faults occurring at different locations along the line: PTGMTR and NTGTR near the terminal of MMC-1 (points F_1 and F_2), PTGMR and NTGMR, at the midpoint of the transmission line (points F_3

and F_4), PTGER and NTGER (points F_5 and F_6), at the end point of line.

Table 3 provides the performance results for the CBTW protection method for overhead lines, including Fault Classification Criteria and internal/external distinction for different fault types. It confirms that the CBTW protection scheme effectively handles all types of internal low-impedance faults but may be inconsistent with high-impedance faults. Additionally, In the context of two-terminal MMC HVDC system, it lacks the ability to ensure selectivity and reliability under external faults. The primary impact of fault distance on traveling wave protection is the attenuation of amplitude and increased propagation time. Fault resistance also reduces the amplitude of traveling waves and subsequently affecting the amplitude-based protection criteria which can be observed from following Table 4.

5. Comparative analysis of PMGMW and CBTW

The quantitative comparison illustrates the strengths and weaknesses of each protection scheme, providing a clear understanding of their performance under different fault conditions. Below is a quantitative comparison between the PMGMW and CBTW protection schemes across various fault scenarios and types.

6. Summary for protection schemes

This research primarily relies on simulation-based analysis, which, while comprehensive, may not fully capture the complexities of real-world operations. The simulations were conducted under idealized conditions, with assumptions such as perfect component behavior and the absence of noise or interference. These factors may influence the performance of the protection schemes in practical settings. Additionally, the study focused on a limited number of fault

Table 3. Summary of CBTW protection scheme.

Fault Type	Fault Location (kms)	Fault Resistance (R_g) in Ω	Integrated value of ΔB (kV)	Correct Operation
Positive Pole to Ground (PTG)	0	0.01	1.26	Yes
	0	100	0.95	Yes
	200	0.01	0.7719	Yes
	200	100	0.548	Yes
	400	0.01	0.5084	Yes
	400	100	0.282	No
	External	0.01	0.0172	No
Negative Pole to Ground (NTG)	0	0.01	-0.020	Yes
	0	100	-0.009	Yes
	200	0.01	-0.0156	Yes
	200	100	-0.016	Yes
	400	0.01	-0.0251	Yes
	400	100	-0.002	No
	External	0.01	0.0144	No
Pole to Pole (PTP)	0	0.01	4.25	Yes
	200	0.01	1.573	Yes
	400	0.01	2.12	Yes
	External	0.01	0.0557	No

Table 4. Backward Travelling wave and its arrival time.

Fault Type	Fault Location (kms)	Fault Resistance (R_g) in Ω	Backward Travelling wave voltage (kV)	Arrival time of Backward Travelling wave (ms)
Positive Pole to Ground (PTG)	0	0.01	651	0.05
	0	100	261	0.06
	200	0.01	462	0.7
	200	100	300	0.75
	400	0.01	367	1.43
	400	100	216	1.45
Negative Pole to Ground (NTG)	0	0.01	661	0.06
	0	100	268	0.07
	200	0.01	463	0.7
	200	100	300	0.75
	400	0.01	347	1.43
	400	100	347	1.45
Pole to Pole (PTP)	0	0.01	2816	0.05
	200	0.01	2279	0.7
	400	0.01	2055	1.43

Table 5. Comparison of PMGMW and CBTW.

	PMGMW	CBTW
Fault Resistance Endurance	Successfully identifies internal faults with fault resistances up to 100 Ω .	Handles internal faults effectively at lower resistances but struggles with higher resistances.
	For a positive pole-to-ground fault at 400 km with 100 Ω resistance, the change in pole mode wave (ΔP) is 0.284 kV and the rate of change of pole mode wave $\frac{dP}{dt}$ is 5.7×10^3 kV/s	For a positive pole-to-ground fault at 400 km with 100 Ω resistance, the integrated value of backward traveling wave (ΔB) is 0.282 kV, which is at the threshold of being detected, indicating potential reliability issues..
	For a negative pole-to-ground fault at 400 km with 100 Ω resistance, the change in pole mode wave (ΔP) is 0.26 kV and the rate of change of pole mode wave $\frac{dP}{dt}$ is 5.2×10^3 kV/s.	For a negative pole-to-ground fault at 400 km with 100 Ω resistance, the integrated value of ΔB is -0.002 kV, which is below the detection threshold, indicating that CBTW protection fails to detect this fault.
Fault Location Accuracy	Demonstrates high accuracy in fault location across different distances.	Also provides high accuracy in fault location but with limitations at higher resistances.
	For example, for a positive pole-to-ground fault at 400 km with 0.01 Ω resistance, the system measures a ground mode wave (G) of 476 kV and a pole mode wave (P) of 367 kV, enabling accurate fault location.	For instance, for a pole-to-pole fault at 400 km with 0.01 Ω resistance, the integrated value of ΔB is 2.12 kV, allowing accurate detection, but for higher resistance, accuracy diminishes.
Processing Time	Generally slower in processing faults due to the comprehensive analysis of multiple criteria.	Faster in detecting faults, particularly in low-resistance scenarios.
	The processing time is longer, which may slightly delay fault isolation but ensures robustness against high-resistance faults.	The processing time is shorter, providing quicker fault isolation, but this comes at the cost of reduced accuracy in high-resistance fault scenarios.
High Resistance Fault Detection	Maintains detection capability even in high-resistance fault scenarios (up to 100 Ω), making it more reliable for a broader range of fault conditions.	Struggles with high-resistance faults; beyond a certain threshold (around 100 Ω at 400 km), the scheme may fail to detect the fault, particularly in PTG/NTG scenarios.
External Fault Differentiation	May or may not detect external faults correctly, especially at large distances (e.g., 400 km), where ΔP and $\frac{dP}{dt}$ exceed thresholds, potentially leading to misidentification.	Similarly, struggles with differentiating external faults, especially at high resistances, where ΔB values can fall within ranges that make detection unreliable.

Table 6. Quantitative Comparison between PMGMW and CBTW.

Fault Type	Fault Location	Fault Resistance (Ω)	Metric	PMGMW	CBTW
Positive Pole to Ground (PTG)	Near Terminal (0 km)	0.01	ΔP (kV)	1.2	N/A
			$\frac{dP}{dt}$ (kV/s)	25.3×10^3	N/A
			ΔB (kV)	N/A	1.26
	Midpoint (200 km)	0.01	ΔP (kV)	0.9	N/A
			$\frac{dP}{dt}$ (kV/s)	17.5×10^3	N/A
			ΔB (kV)	N/A	0.7719
	End Point (400 km)	0.01	ΔP (kV)	0.56	N/A
			$\frac{dP}{dt}$ (kV/s)	11.33×10^3	N/A
			ΔB (kV)	N/A	0.5084
Positive Pole to Ground (PTG)	Near Terminal (0 km)	100	ΔP (kV)	0.4	N/A
			$\frac{dP}{dt}$ (kV/s)	8×10^3	N/A
			ΔB (kV)	N/A	0.95
	End Point (400 km)	100	ΔP (kV)	0.284	N/A
			$\frac{dP}{dt}$ (kV/s)	5.7×10^3	N/A
			ΔB (kV)	N/A	0.282
Negative Pole to Ground (NTG)	Near Terminal (0 km)	0.01	ΔP (kV)	1.28	N/A
			$\frac{dP}{dt}$ (kV/s)	25.6×10^3	N/A
			ΔB (kV)	N/A	-0.02
	Midpoint (200 km)	100	ΔP (kV)	0.5	N/A
			$\frac{dP}{dt}$ (kV/s)	9.9×10^3	N/A
			ΔB (kV)	N/A	-0.016
	End Point (400 km)	100	ΔP (kV)	0.26	N/A
			$\frac{dP}{dt}$ (kV/s)	5.2×10^3	N/A
			ΔB (kV)	N/A	-0.002 (Failed)
Pole to Pole (PTP)	Near Terminal (0 km)	0.01	ΔP (kV)	6.02	N/A
			$\frac{dP}{dt}$ (kV/s)	120×10^3	N/A
			ΔB (kV)	N/A	4.25
	Midpoint (200 km)	0.01	ΔP (kV)	5.56	N/A
			$\frac{dP}{dt}$ (kV/s)	98.5×10^3	N/A
			ΔB (kV)	N/A	1.573
	End Point (400 km)	0.01	ΔP (kV)	6.85	N/A
			$\frac{dP}{dt}$ (kV/s)	137×10^3	N/A
			ΔB (kV)	N/A	2.12

	PMGMW	CBTW
Processing Time	It has a longer processing time due to the comprehensive analysis of multiple criteria, such as ΔP , $\frac{dP}{dt}$ and $\frac{dG}{dt}$. This thorough approach ensures reliability, particularly in high-resistance fault scenarios, but it slightly delays the fault isolation process. The exact processing times are not explicitly provided in the figures but can be inferred as being slower compared to CBTW.	It is designed for faster fault detection, particularly effective in low-resistance fault scenarios. The faster processing is achieved by focusing on the rate of change of voltage (ROCOV) and the integral value of ΔB within a short time window (10 milliseconds). The figures suggest that CBTW scheme can detect faults almost immediately after they occur, especially in scenarios with low resistance, making it quicker but less robust in certain high-resistance conditions.
Accuracy	This protection shows high accuracy in identifying fault locations and types across various scenarios, including high-resistance faults. For example, in a PTG fault at 400 km with 100 Ω resistance, the scheme successfully identifies the fault with $\Delta P = 0.284$ kV and $\frac{dP}{dt} = 5.7 \times 10^3$ kV/s, demonstrating its reliability even in challenging conditions	This protection provides accurate fault detection in low-resistance scenarios but struggles with high-resistance faults. For instance, in an NTG fault at 400 km with 100 Ω resistance, the ΔB value is -0.002 kV, which is below the detection threshold, resulting in a failure to detect the fault. However, in low-resistance scenarios, such as a PTP fault at 400 km with 0.01 Ω resistance, the ΔB value of 2.12 kV indicates accurate detection.

Table 7. Summary Table of Key Metrics.

Metric	PMGMW Protection	CBTW Protection
Max Fault Resistance (Internal)	100 Ω (Reliable)	Up to 100 Ω (Unreliable for negative pole)
Processing Time	Slower (More thorough analysis)	Faster (Quicker fault isolation)
Accuracy at 400 km, 0.01 Ω	$\Delta P = 0.56$ kV, $dP/dt = 11.33 \times 10^3$ kV/s	$\Delta B = 2.12$ kV (Reliable for PTP faults)
Accuracy at 400 km, 100 Ω	$\Delta P = 0.284$ kV, $dP/dt = 5.7 \times 10^3$ kV/s	$\Delta B = 0.282$ kV (Unreliable)
External Fault Detection	May misidentify at large distances	Inconsistent, particularly in high resistance scenarios

scenarios and did not explore multi-terminal HVDC systems or varying environmental conditions. As such, the findings may require further validation through field tests or more complex simulations incorporating real-world disturbances and system variances.

This study analyzes and compares the performance of traveling wave protection by CBTW and PMGMW of LCC HVDC system to two terminal MMC HVDC system based on transition resistance, fault distance, internal and external faults. The findings indicate that PMGMW protection demonstrates a higher tolerance to transition resistance than CBTW protection. Both CBTW and PMGMW traveling wave protection schemes utilize rate-of-change criteria to enhance fault discrimination. CBTW employs change in fault generated backward travelling wave for fault line selection, whereas PMGMW utilizes the rate of change of ground mode component for this purpose. To address the limitations of traveling wave protection schemes for DC line by both PMGMW and CBTW, an improvement points are proposed based on existing criteria. These research outcomes are valuable for operation and maintenance personnel in understanding and enhancing traveling wave protection technology for MMC HVDC lines.

1) Speed takes precedence when safeguarding MMC HVDC grids, unlike AC power systems and LCC-HVDC systems. Consequently, ultra-high-speed single-end protection schemes are predominantly chosen. A high sampling frequency is essential to uphold the reliability of single-end protection, ensuring an effective balance between speed and sensitivity.

2) Modal-domain analysis decouples positive and negative pole interactions to analyze asymmetric faults. It uses zero-mode for faulted pole selection and line-mode for internal faults. Time-domain analysis studies traveling wave propagation revealing voltage and current variations for external versus internal faults. Frequency-domain analysis identifies high-frequency components in transient currents and voltages which is difficult for time domain analysis.

3) Present single-end protection schemes commonly use boundary protection with large current-limiting inductors for selectivity and sensitivity. These methods include time-domain traveling wave (TW) approaches, signal processing techniques, and voltage-based methods with current-limiting inductors. To improve performance in weaker boundary conditions, research is required for single-end protection schemes independent of boundary effects.

4) Protection should be robust, accurate and fast. It should not be affected by fault resistance and noise interference. Signal processing tool like FFT, Wavelet Transform etc. can effectively overcome mentioned issue.

5) A suitable DC direction criterion for MMC HVDC grids, particularly one that does not rely on boundary components, remains to be developed. The enhanced transient traveling wave-based directional criterion, which does not rely on boundary components and is unaffected by the frequency-dependent characteristics of DC line parameters, can be used.

6) The recognition of both internal and external faults relies on detection of high-frequency voltage components. Thus, it is imperative to employ signal processing techniques that are adept at extracting these high-frequency components effectively.

7. Conclusion

The performance of CBTW's and PMGMW's travelling wave-based protection schemes was evaluated using a variety of criteria, such as fault resistance handling, fault location accuracy, and processing time." PMGMW's protection scheme exhibited exceptional fault resistance endurance, effectively identifying faults with resistances as high as 100 Ω , thereby increasing its reliability in scenarios with high-resistance faults. Nevertheless, it demonstrated extended processing periods in comparison to CBTW's scheme, which was more efficient in fault detection but less effective in distinguishing high-resistance faults. The two schemes demonstrated comparable fault location accuracy, with both demonstrating high precision in identifying fault locations across a range of distances. In the selection of suitable protection mechanisms for MMC HVDC systems, the trade-offs between speed and robustness are emphasized by these results. Thus, PMGMW Protection offers High accuracy in high-resistance fault detection, robust fault location capabilities against slower processing time, potential misidentification of external faults at long distances. Whereas, CBTW Protection offers faster processing time, and seems effective in low-resistance scenarios against lower accuracy in high-resistance fault detection, particularly with PTG/NTG faults at long distances. This detailed comparison provides a clear understanding of the trade-offs between processing speed and accuracy in the two protection schemes, highlighting their suitability for different operational contexts in MMC HVDC systems. Additionally, the paper suggests modifications to the algorithmic thresholds and processing steps, optimizing the balance between speed and reliability. These enhancements address critical challenges in current protection systems that attempts to offer a more robust solution for modern HVDC grids.

8. Nomenclature

PMGMW- Pole Mode Ground Mode Wave
 CBTW- Change in Backward Travelling Wave
 PTGT- Positive Pole to Ground fault at Terminal
 NTGT- Negative Pole to Ground fault at Terminal
 PTPT- Pole to Pole Fault at Terminal
 PTGTR- Positive Pole to Ground Fault at terminal with R
 NTGTR- Negative Pole to Ground Fault at Terminal with R
 PTGM- Positive Pole to Ground fault at Mid Point
 NTGM- Negative Pole to Ground fault at Mid Point
 PTPM- Pole to Pole Fault at Mid Point
 PTGMR- Positive Pole to Ground Fault at Mid Point with R
 NTGMR- Negative Pole to Ground Fault at Mid Point with R
 PTGE- Positive Pole to Ground fault at End Point
 NTGE- Negative Pole to Ground fault at End Point
 PTPE- Pole to Pole Fault at End Point
 PTGER- Positive Pole to Ground Fault at End Point with R
 NTGER- Negative Pole to Ground Fault at End Point with R

Data availability

Data underlying the results presented in this paper are available from the corresponding author upon reasonable request.

Funding

There is no funding for this work.

Conflicts of interest

The authors declare no conflict of interest.

Ethics

The authors declare that the present research work has fulfilled all relevant ethical guidelines required by COPE.

Authors contributions

Authors have contributed equally in preparing and writing the manuscript.

Availability of data and materials

The authors declare that the data supporting the findings of this study are available within the paper.

Conflict of interests

The authors declare that they have no known competing financial interests or personal relationships that could have appeared to influence the work reported in this paper.

Open access

This article is licensed under a Creative Commons Attribution 4.0 International License, which permits use, sharing, adaptation, distribution and reproduction in any medium or format, as long as you give appropriate credit to the original author(s) and the source, provide a link to the Creative Commons license, and indicate if changes were made. The images or other third party material in this article are included in the article's Creative Commons license, unless indicated otherwise in a credit line to the material. If material is not included in the article's Creative Commons license and your intended use is not permitted by statutory regulation or exceeds the permitted use, you will need to obtain permission directly from the OICC Press publisher. To view a copy of this license, visit <https://creativecommons.org/licenses/by/4.0>.

References

- [1] B. Li, J. He, and J. Tian. "DC fault analysis for modular multilevel converter-based system." 5(2):275–282, 2015. DOI: <https://doi.org/10.1007/s40565-015-0174-3>.
- [2] F. Kong, Z. Hao, S. Zhang, and B. Zhang. "Development of a Novel Protection Device for Bipolar HVDC Transmission Lines." 29(5), 2014. DOI: <https://doi.org/10.1109/tpwr.2014.2305660>.
- [3] Y. J. Ma, H. F. Li, and J. B. Hu. "Study on fault travelling wave characteristics in double-circuit HVDC." *Power and Energy Engineering Conference*, 2013. URL <https://en.cnki.com.cn/Article-en/CJFDTOTAL-JDQW201423011.htm>.
- [4] Z. Li, G. B. Zou, and B. B. Tong. "Novel traveling wave protection method for high voltage DC transmission line." *IEEE Power & Energy Society General Meeting*, 2015. DOI: <https://doi.org/10.1109/pesgm.2015.7285910>.
- [5] A. Li, Z. Cai, Q. Sun, X. Li, D. Renand, and Z. Yang. "Analysis on the Dynamic Performance Characteristics of HVDC Control and Protections for the HVDC Line Faults." *IEEE Power Energy Society General Meeting*, pages 1–5, 2009. DOI: <https://doi.org/10.1109/PES.2009.5275974>.
- [6] J. Descloux, B. Raisonand, and J. B. Curis. "Protection algorithm based on differential voltage measurement for MTDC grids." *IET International Conference on Developments in Power System Protection*, pages 1–5, 2014. DOI: <https://doi.org/10.1049/cp.2014.0010>.
- [7] K. De Kerf. "Wavelet-based protection strategy for DC faults in multi-terminal VSC HVDC systems." *IET*, 5(4), 2011. DOI: <https://doi.org/10.1049/iet-gtd.2010.0587>.
- [8] J. Sneath and A. Rajapakse. "Fault Detection and Interruption in an Earthed HVDC Grid Using ROCOV and Hybrid DC Breakers." *IEEE Transaction on Power Delivery*, 31(3), 2016. DOI: <https://doi.org/10.1109/TPWRD.2014.2364547>.
- [9] R. Li, L. Xu, and L. Yao. "DC Fault Detection and Location in Meshed Multiterminal HVDC Systems Based on DC Reactor Voltage Change Rate." *IEEE Transaction on Power Delivery*, 32(3), 2017. DOI: <https://doi.org/10.1109/TPWRD.2016.2590501>.
- [10] W. Leterme, J. Beerten, and D. Van Hertem. "Non unit Protection of HVDC Grids With Inductive DC Cable Termination." *IEEE Transaction on Power Delivery*, 31(2), 2016. DOI: <https://doi.org/10.1109/TPWRD.2015.2422145>.
- [11] J. Liu, N. Taiand, and C. Fan. "Transient-Voltage-Based Protection Scheme for DC Line Faults in the Multiterminal VSC-HVDC System." *IEEE Transaction Power on Delivery*, 32(3), 2017. DOI: <https://doi.org/10.1109/TPWRD.2016.2608986>.
- [12] W. Xiang, S. Yang, L. Xu, J. Zhang, W. Linand, and J. Wen. "A Transient Voltage-Based DC Fault Line Protection Scheme for MMC-Based DC Grid Embedding DC Breakers." *IEEE Transaction Power on Delivery*, 34(1), 2019. DOI: <https://doi.org/10.1109/TPWRD.2018.2874817>.
- [13] N. Geddada, Y. M. Yeapand, and A. Ukil. "Experimental Validation of Fault Identification in VSC-Based DC Grid System." *IEEE Transaction on Industrial Electronics*, 65(6), 2018. DOI: <https://doi.org/10.1109/TIE.2017.2767560>.
- [14] R. Derakhshanfar, T. U. Jonsson, U. Steigerand, and M. Habert. "Hybrid HVDC breaker-A solution for future HVDC system." *CIGRE Session*, pages 1–12, 2014.
- [15] C. Li, C. Zhao, J. Xu, J. Yuke, Z. Fanand, and T. An. "A Pole-to-Pole Short-Circuit Fault Current Calculation Method for DC Grids." *IEEE Transaction on Power Systems*, 32(6), 2017. DOI: <https://doi.org/10.1109/TPWRS.2017.2682110>.

- [16] R. Vidal-Albalade, H. Beltrán, A. Rolan, E. Belenguer, R. Penaand, and R. Blasco-Gimenez. “**Analysis of the Performance of MMC Under Fault Conditions in HVDC-Based Offshore Wind Farms.**”. *IEEE Transaction Power on Delivery*, 31(2), 2016. DOI: <https://doi.org/10.1109/TPWRD.2015.2468171>.
- [17] L. Liu, A. Leki´c, and M. Popov. “**Robust Traveling Wave-Based Protection Scheme for Multi terminal DC Grids.**”. *IEEE Transaction Power on Delivery*, 38(5), 2023. DOI: <https://doi.org/10.1109/TPWRD.2023.3265748>.
- [18] R. Hussain, F. Akhter, J. B. Soomro, and J. A. Ansari. “**Control and protection of MMC-based HVDC systems: A review.**”. *Energy Reports*, 9(12), 2023. DOI: <https://doi.org/10.1016/j.egyr.2022.12.056>.
- [19] C. Zhang, G. Song, A. S. Meliopoulosand, and X. Dong. “**Setting-Less Non unit Protection Method for DC Line Faults in VSC-MTdc Systems.**”. *IEEE Transaction on Industrial Electronics*, 69(1), 2022. DOI: <https://doi.org/10.1109/TIE.2021.3050380>.
- [20] W. Zheng, N. Zhangand, and G. Y. Yang. “**Comparative and improvement investigation on the DC transmission line traveling wave protections of Siemens and ABB.**”. *Power System Protection and Control*, 43(24):149–154, 2015.
- [21] C. Zhang, G. Song, T. Wangand, and X. Dong. “**An Improved Non-Unit Traveling Wave Protection Method With Adaptive Threshold Value and Its Application in HVDC Grids.**”. *IEEE Transaction Power on Delivery*, 35(4), 2020. DOI: <https://doi.org/10.1109/TPWRD.2019.2954599>.